

# Infrared Studies on Polymorphs of Silicon Dioxide and Germanium Dioxide

Ellis R. Lippincott,<sup>1</sup> Alvin Van Valkenburg, Charles E. Weir, and Elmer N. Bunting

The infrared spectra of coesite, low-temperature tridymite, low-temperature cristobalite-low-temperature quartz, vitreous silica, hexagonal  $\text{GeO}_2$ , tetragonal  $\text{GeO}_2$ , and vitreous germania are reported from 4,000 to 300  $\text{cm}^{-1}$ . Wherever possible an assignment of frequencies has been made on the basis of the selection rules for the crystal symmetry. Three characteristic group frequencies near 1,100, 800, and 480  $\text{cm}^{-1}$  are common to all the polymorphs of  $\text{SiO}_2$ . These frequencies respectively correspond to a stretching mode involving displacements associated primarily with the oxygen atoms, a stretching mode involving displacements associated primarily with the silicon atoms, and a Si-O bending mode. The presence of these group frequencies in coesite indicates that the coordination of silicon in coesite is tetrahedral and that its high density is associated with the packing of tetrahedral units at an angle approximating 120 degrees. The tetragonal and hexagonal  $\text{GeO}_2$  polymorphs show a marked difference in spectra due in part to the change from sixfold to fourfold coordination. The assignment of observed frequencies in hexagonal  $\text{GeO}_2$  is consistent with that made for low-temperature quartz if allowance is made for the heavier mass of the Ge atom.

## 1. Introduction

Several investigators have presented a detailed analysis of the vibrational spectrum of quartz [1].<sup>2</sup> Infrared spectra of cristobalite and fused silica have been reported but no specific assignments of their spectra appear to have been given [1]. Infrared spectra are presented of the  $\text{SiO}_2$  polymorphs of coesite, cristobalite, tridymite, and vitreous silica; also the  $\text{GeO}_2$  polymorphs of hexagonal  $\text{GeO}_2$ , tetragonal  $\text{GeO}_2$ , and vitreous  $\text{GeO}_2$ , in the region from 4,000  $\text{cm}^{-1}$  to 300  $\text{cm}^{-1}$ . A partial interpretation of the spectra in terms of respective structures and selection rules is given. Particular emphasis has been placed on locating characteristic frequencies and on classifying the observed frequencies in terms of types of vibrations. The assignment of frequencies is admittedly tentative in part because either the true crystal symmetry is not known, the spectral data are incomplete, or the spectra are too complex. Because coordination of silicon in coesite [2] has not been established, one of the objectives of this work was to furnish evidence for either the fourfold coordination of the other polymorphs of  $\text{SiO}_2$  or for a different coordination. In the tetragonal form of  $\text{GeO}_2$  the germanium atom has a sixfold coordination with oxygen, whereas in the quartz-type hexagonal  $\text{GeO}_2$  the germanium atom has the fourfold coordination of silicon in quartz [3, 4]. A similar tetragonal form of silica is not known but has been predicted by analogy with germania.

## 2. Experimental Procedure

### 2.1. Samples

The cristobalite was prepared from  $\gamma$ -ethyl orthosilicate by the usual hydrolysis technique. The  $\text{SiO}_2$  thus obtained was heated to 1,600°C for 5 hr. Its

X-ray powder pattern was identical with that found for natural cristobalite. A quartz sample of high purity was obtained from the Geophysical Laboratory (standard sample). Crystals of coesite were prepared from precipitated silicic acid which was subjected to 30,000 atm at 600°C for one-half hour. The X-ray powder pattern and indices of refraction of this material agree with those reported by Coes [2]. Tridymite was prepared by C. N. Fenner of the Geophysical Laboratory. The preparation was accomplished by heating pure quartz and  $\text{Na}_2\text{WO}_4$  at 1,000°C for 71 hr, followed by careful purification of the tridymite. The fused silica was obtained by fusing a sample of pure quartz in the usual manner.

The germanium oxide was obtained commercially. Microscopic examination showed extremely fine particles less than 1  $\mu$  in size. X-ray powder patterns of the material coincided with those reported for the hexagonal form of  $\text{GeO}_2$  [4]. The tetragonal form of  $\text{GeO}_2$  was prepared hydrothermally. The hexagonal  $\text{GeO}_2$  was sealed with water in a platinum capsule and heated at 800°C at a pressure of 20,000 psi for 3 days. Microscopic examination showed some crystal growth of tetragonal  $\text{GeO}_2$ , but crystals were still too small (circa 1  $\mu$ ) to permit more than an estimation of the index, approximately 1.99. X-ray patterns showed tetragonal  $\text{GeO}_2$  with a small amount—estimated at less than 5 percent—of unconverted hexagonal material. Spectroscopic analysis of the tetragonal material showed principal impurities to be Pt 0.1 to 1.0 percent; Al, Ca, Fe, Pd, and Si 0.01 to 0.1 percent; and smaller quantities of Ag, Ba, Cu, Mg, Mn, and Pb, which were found as traces. Vitreous  $\text{GeO}_2$  was formed by quenching fused hexagonal  $\text{GeO}_2$  in a platinum container.

### 2.2. Infrared Studies

Infrared spectra of the samples were obtained on a double-beam spectrophotometer with NaCl prism in the region 4,000 to 650  $\text{cm}^{-1}$  and on a single-beam double-pass spectrophotometer with CsBr prism in the region 700 to 300  $\text{cm}^{-1}$ . The samples were

<sup>1</sup> Consultant to the Mineral Products Division, National Bureau of Standards. Present address, Department of Chemistry, University of Maryland, College Park, Maryland.

<sup>2</sup> Figures in brackets indicate the literature references at the end of this paper.

ground in a boron carbide mortar, mixed with dry ground KBr and pressed into KBr pellets at 100,000 psi by standard techniques [5]. The concentrations range from 2 to 3 mg of sample per gram of KBr. The spectra from 4,000  $\text{cm}^{-1}$  to 300  $\text{cm}^{-1}$  are given in figures 1 to 15. The region above 1,500  $\text{cm}^{-1}$  contained no fundamental frequencies for any of the polymorphs of  $\text{SiO}_2$  or  $\text{GeO}_2$ . Absorption peaks near 3,500  $\text{cm}^{-1}$  were due to water present in the KBr. The observed frequencies given in figures 1 to 15 are tabulated in tables 2, 4, 5, 7, 8, and 9.

### 3. Interpretations

A  $\text{SiO}_2$  group in a rigid framework has  $3N-3$  or six vibrational degrees of freedom. There is some ambiguity as to how the corresponding modes of vibration should be classified in terms of bond stretching, bond bending, and bond-distortion types. Somewhat arbitrarily a bond-stretching and bond-bending mode will be associated with each O atom. These O-stretching modes should correspond to the highest observed frequencies in the spectrum. Two remaining degrees of freedom need to be assigned to the Si atom. One of these must be a stretching mode corresponding approximately to motions of the Si atom between the two O atoms. The one remaining mode must correspond to a low-frequency distortion or bending motion of the Si atom.

For each  $\text{SiO}_2$  group which is added to the first to make up the unit cell, one must add nine vibrational degrees of freedom. These nine modes may be classified approximately into the following types. Because each added  $\text{SiO}_2$  group corresponds to the addition of four bonds, four of the nine modes correspond to bond-stretching frequencies, two involving displacements associated with the O atoms and two for the Si atom. (Using another description these would correspond to two antisymmetric stretching modes of the type  $\leftarrow\text{Si O}\rightarrow\leftarrow\text{Si}$ , and two symmetric stretching modes of the type  $\leftarrow\text{Si O Si}\rightarrow$ .) Two more of these nine modes may be classified as bending motions associated with the bending of Si-O-Si angle. The remaining three modes are associated with low-frequency bending or distortion frequencies. Table 1 summarizes this classification of the modes of vibration for various numbers of  $\text{SiO}_2$  groups per unit cell. The case for  $N$  equal to

3 corresponds to quartz and that for  $N$  equal to 8 to cristobalite. It should be emphasized that this classification into types is only approximate and that in general a given mode will be a mixture of stretching, bending, and distortions types. The proper method of classifying these modes would be in terms of the symmetry elements of the crystal. For quartz this has been impressively illustrated by Saksena [1]. Because there is some doubt as to the true crystal symmetry of cristobalite, and that of coesite [2] has not been described in detail, this method of classifying normal modes on the basis of symmetry is not possible at the present time for these latter two forms of silica.

The feasibility of the method outlined above for the classifications of the normal modes of various forms of silica may be tested on the assignment given for quartz by Saksena [1]. From table 1 one would expect, in order of decreasing frequency, four distinct spectral groupings consisting of six Si-O stretching modes involving displacements associated primarily with the O atoms, five stretching modes involving displacements associated primarily with the silicon atom, six Si-O-Si bending modes and seven low-frequency distortion modes. These are readily associated with the frequencies observed in the following regions of the spectrum: 1,200 to 1,000  $\text{cm}^{-1}$ , 825 to 600  $\text{cm}^{-1}$ , 600 to 390  $\text{cm}^{-1}$ , and 380 to 100  $\text{cm}^{-1}$ , respectively. The distinction between the latter two groupings is somewhat arbitrary. If one allows for the fact that frequencies assigned to species E in table 2 must be counted twice because they are doubly degenerate, it is found that these groupings contain 6, 5, 6, and 7 degrees of freedom, respectively, in agreement with the numbers expected from a unit cell containing three  $\text{SiO}_2$  groups.

#### 3.1. Cristobalite

The observed spectra were taken on low-temperature  $\alpha$ -cristobalite. Since little information is available about its structure, the spectra are interpreted on the basis of that for high cristobalite for which more structural information is available [6, 7]. High cristobalite was studied by Wyckoff for which he proposed a cubic structure of space-group symmetry  $O_h^7 = \text{Fd}\bar{3}\text{m}$  with eight  $\text{SiO}_2$  groups per unit cell [6]. Application of  $O_h$  selection rules shows that only 5 triply degenerate fundamental frequencies of species  $F_{1u}$  corresponding to 15 of the 69 modes of vibration for the unit cell should appear in the infrared spectrum. Because the observed spectrum of low-temperature cristobalite contains at least seven frequencies plus additional low-frequency peaks below 300  $\text{cm}^{-1}$ , it is not feasible to interpret the infrared spectrum on the basis of  $O_h^7 = \text{Fd}\bar{3}\text{m}$  space-group symmetry. Barth [7] reexamined the structure of high temperature  $\beta$ -cristobalite and concluded that its structure corresponded to a lower symmetry and proposed a structure with space-group symmetry  $T^4 = \text{P}2_13$ . Application of T-selection rules to a unit cell with eight  $\text{SiO}_2$  units predicts that seventeen triply degenerate fundamental frequencies should be observed in the infrared spectrum. At least twelve

TABLE 1. Descriptive classification of the modes of vibration for different numbers of  $\text{SiO}_2$  groups per unit cell

	SiO <sub>2</sub> groups per unit cell						Spectral region assigned for polymorphs of SiO <sub>2</sub> .
	1	2	3	4	6	8	
Number of Si-O stretching modes involving motion primarily associated with the oxygen atoms.	2	4	6	8	12	16	1,200 to 1,000 $\text{cm}^{-1}$ .
Number of stretching modes involving motion primarily associated with the silicon atoms.	1	3	5	7	11	15	825 to 600 $\text{cm}^{-1}$ .
Si-O bending modes.....	2	4	6	8	12	16	600 to 390 $\text{cm}^{-1}$ .
Distortion modes.....	1	4	7	10	16	22	380 to 100 $\text{cm}^{-1}$ .
Total modes.....	6	15	24	33	51	69	

TABLE 2. Classification of fundamental frequencies ( $\text{cm}^{-1}$ ) in  $\alpha$ -Quartz

Species	Spectral activity	Saksena <sup>a</sup>	Kirshman <sup>a</sup>	Barriol <sup>a</sup>	Simons and McMahon <sup>a</sup>	This work <sup>b</sup>	Descriptive assignment
A	Raman-----	207	207	207	-----	(207)	Distortion.
		356	258	356	-----	(356)	Distortion.
		466	467	466	-----	(466)	Si-O bending.
		1,082	1,082	1,082	-----	(1,082)	Si-O stretching.
B	Infrared with no dipole // Z <sup>c</sup> -----	364	378	385	-----	374	Distortion.
		508	480	488	-----	513	Si-O bending.
		777	805	800	-----	780	Si stretching.
		1,149	-----	1,190, 1,227	-----	1,150	Si-O stretching.
		128	127	127	-----	(128)	Distortion.
		392 to 403	404	394	-----	397	Si-O bending.
E <sup>d</sup>	Infrared with no dipole // Z <sup>c</sup> -----	695	696	696	-----	696	Si stretching.
		1,159	1,160	1,163	-----	1,176	Si-O stretching.
		265	267	268	-----	(265)	Distortion.
		479	-----	-----	-----	462 to 475	Si-O bending.
		795 to 807	794	798	-----	801	Si stretching.
-----	1,063	1,065	-----	1,097	Si-O stretching.		
-----	-----	1,228	1,228	-----	-----	-----	

<sup>a</sup> See reference in text. <sup>b</sup> Figures in parentheses indicate the use of Saksena's assignment. <sup>c</sup> Direction of optic axis. <sup>d</sup> Species E is doubly degenerate and the observed frequencies correspond to two modes.

of these should be observed in the region above 300  $\text{cm}^{-1}$ , and it is considered unlikely that a satisfactory interpretation of the spectrum can be made on the basis of space-group symmetry  $T^4 = P2_13$ .

These considerations suggest that a tentative assignment and classification of observed frequencies may be made on the basis of a different symmetry which has vibrational selection rules not as stringent as an  $O_h$  structure but more restrictive than a T structure. To accomplish this, the  $T_d$  selection rules are assumed to be of approximate value [8]. The vibrational species for a structure of  $T_d$  symmetry are  $A_1, A_2, E, F_1$  and  $F_2$ . Of these the only species which is infrared active is  $F_2$ . Ten fundamental triply degenerate infrared frequencies are predicted, of which eight should appear in the region above 300  $\text{cm}^{-1}$ . This latter number corresponds closely with the number of observed frequencies. In table 3 are summarized the distribution of Si-O stretching, Si stretching, Si-O bending, and low-frequency distortion modes among the vibrational species for a structure of  $T_d$  symmetry. The three Si-O stretching modes may be assigned to the peaks observed at 1,204, 1,160 and 1,104  $\text{cm}^{-1}$ , respectively. The two Si stretching modes involving displacements associated primarily with motion of the Si atoms may be assigned to the peaks observed at 798 and 620  $\text{cm}^{-1}$ , respectively. The three bending modes have been assigned to the bands observed near 515 and 485  $\text{cm}^{-1}$ . The two infrared active distortion modes are expected in the 150 to 200  $\text{cm}^{-1}$  region and would not be observed. The classification given in table 4, based on assumed  $T_d$  selection rules and group frequencies, explains the fact that the observed spectrum is simpler than that of quartz and enables one to obtain a tentative assignment of all the observed frequencies.

A more detailed and complete assignment for cristobalite must await the obtaining of a Raman spectrum and additional infrared studies at longer wavelengths on single crystals, followed by an analysis based on the true crystal symmetry.

A comparison of the spectra of quartz and of cristobalite shows that the most intense component of the Si-O antisymmetric stretching frequencies

TABLE 3. Selection rules and group frequency classification for a  $T_d$  structure with 8  $\text{SiO}_2$  groups per unit cell

Species <sup>a</sup>	Spectral activity	Total frequencies	Si-O stretchings	Si stretchings	Si-O bendings	Low frequency distortions
$A_1$ ----	Raman-----	5	2	1	2	-----
$A_2$ ----	Inactive-----	1	-----	-----	-----	1
E-----	Raman-----	6	1	1	1	3
$F_1$ ----	Inactive-----	7	1	2	1	3
$F_2$ ----	Infrared and Raman.	10	3	2	3	2

<sup>a</sup>The E and F species are doubly and triply degenerate and the corresponding frequencies must be counted two and three times, respectively.

TABLE 4. Classification of observed infrared frequencies for cristobalite <sup>a</sup>

$\text{cm}^{-1}$	Description
485	Si-O bending.
515	Si-O bending.
620	Si stretching.
798	Si stretching.
1,104	Si-O stretching.
1,160	Si-O stretching.
1,204	Si-O stretching.

<sup>a</sup>  $F_2$  is the only active infrared species for  $T_d$  symmetry. The Raman active species are  $A_1, E_2$ , and  $F_2$ .

differs by only 7  $\text{cm}^{-1}$ , with the peak for cristobalite being at the larger  $\text{cm}^{-1}$  value. This result is somewhat different from that found by Simmons and McMahon [1] with infrared reflection studies, where the Si-O stretching frequency was found at different  $\text{cm}^{-1}$  values for quartz, cristobalite, and fused silica. Likewise the Si stretching frequencies near 800  $\text{cm}^{-1}$  do not differ greatly between the two forms. The only other frequencies that appear to be somewhat the same in both forms are those that correspond to the strong peaks occurring in the region 460 to 515  $\text{cm}^{-1}$ . These frequencies have been assigned to a mixed Si-O-Si and O-Si-O bending mode. However, corresponding low-frequency peaks in quartz are definitely shifted to lower frequencies from their counterparts in cristobalite. This shift will be

tentatively associated with the change in angle that the tetrahedral units make with each other in the respective structures. The fact that the Si and Si-O stretching frequencies occur at nearly the same positions, respectively, in both compounds indicates that the difference in structure between the two is associated with the orientation of the tetrahedral unit rather than any great difference between Si-O bond distances or Si-O bond-stretching force constants, resulting from a change of coordination.

### 3.2. Coesite

The infrared spectrum of coesite given in figure 3 and tabulated in table 5 is richer and more complex than that for either quartz or cristobalite. This is expected since the crystal symmetry of coesite [2] is lower (space group  $\bar{C}c$  or  $C2/c$ ) and has 16 to 18  $\text{SiO}_2$  groups per unit cell. Two factors make it difficult to obtain an assignment of frequencies for coesite. First, the exact crystal symmetry is not known, nor can a pseudo structure of high symmetry be assumed to simplify the analysis. Second, the exact number of  $\text{SiO}_2$  groups per unit cell is uncertain. However, the infrared spectrum of coesite shows the presence of group frequencies similar to those found in quartz and cristobalite. The Si-O stretching frequencies appear near  $1,100\text{ cm}^{-1}$  whereas the Si stretching frequencies appear near  $800\text{ cm}^{-1}$ . This indicates that the tetrahedral unit in coesite is still intact and that there has been no change in coordination of the Si atom or marked change in Si-O bond length or marked change in Si-O bond stretching-force constant. (It is interesting that this is not the case for the hexagonal and tetragonal forms of  $\text{GeO}_2$ .) The difference in structure appears to be due to the packing of the tetrahedral units. Evidence for this is that the mixed Si-O-Si and O-Si-O bending frequencies, which appear at  $515$  and  $485\text{ cm}^{-1}$  in cristobalite and at  $475$  and  $462\text{ cm}^{-1}$  in quartz, shift to  $442$  and  $430$  in coesite. We interpret this shift to be associated with the change in angle between the tetrahedral units of the three structures. Empirically one may estimate this angle in coesite by correlating this shift with the known angles in cristobalite and quartz, which are near  $180^\circ$  and  $150^\circ$ , respectively. This indicates that this angle in coesite is approximately  $120^\circ \pm 10^\circ$ .

TABLE 5. Classification of observed infrared frequencies of coesite

$\text{cm}^{-1}$	Description
340	Distortion.
390	} Si-O-Si and O-Si-O bending.
430	
442	
557	
598	
683	} Si stretching ( $\leftarrow\text{Si-O-Si}\rightarrow$ ).
796	
813	
1,040	} Si-O stretching ( $\leftarrow\text{Si O}\rightarrow\leftarrow\text{Si}$ ).
1,098	
1,170	
1,225	

### 3.3. Low-Temperature Tridymite

Low-temperature tridymite forms orthorhombic crystals with 64  $\text{SiO}_2$  groups per unit cell [9]. The true crystal symmetry is not known, but it is believed to be a distorted form of the simpler high-temperature  $\beta$ -tridymite, which has a simple hexagonal structure of  $D_{3h}^4=C\bar{6}2c$  or  $D_{3h}^4=C6/mmc$  space-group symmetry. In order to obtain an approximate interpretation of the infrared spectrum of the low-temperature tridymite it is assumed that the selection rules for the high-temperature tridymite of  $D_{3h}^4$  symmetry are approximately valid despite the fact that the true symmetry is a distortion of the  $D_{3h}^4$  symmetry. The infrared active species are  $A_2'$  and  $E'$  corresponding to nine fundamental frequencies ( $4A_2''$  and  $5E_1'$ ). The  $D_{3h}$  selection rules [8] and a classification of Si-O stretching, Si stretching, Si-O bending, and low-frequency distortion modes are given in table 6. The two Si-O stretching modes in species  $A_2''$  have been assigned to the peaks observed at  $1,109$  and  $1,175\text{ cm}^{-1}$ . The  $A_2''$  Si-O bending mode has been assigned to the  $478\text{ cm}^{-1}$  peaks. The distortion mode in  $A_2''$  would be expected near  $200\text{ cm}^{-1}$  and has not been observed. The five frequencies of species  $E'$  have been classified as corresponding to an Si-O stretching, an Si stretching, two Si-O bendings, and a distortion mode. The Si-O stretching has been assigned at  $1,109\text{ cm}^{-1}$ , the Si stretching at  $792\text{ cm}^{-1}$  and the two Si-O bendings to the  $478\text{ cm}^{-1}$  peak and its nearby component. The low-frequency distortion would be expected in the  $150$  to  $200\text{ cm}^{-1}$  regions and would be missed by the instruments used in this work.

TABLE 6. Selection rules and classification of modes of vibration for tridymite assuming space group  $D_{3h}^4=C\bar{6}2c$

Species <sup>a</sup>	Spectral activity	Total frequencies	Si-O stretchings	Si stretchings	Si-O bending	Low frequency distortions
$A_2'$	Raman	5	2	1	1	1
$A_1'$	Inactive	1	-----	-----	-----	1
$A_2''$	Inactive	1	-----	-----	-----	1
$A_2''$	Infrared	4	2	-----	1	1
$E'$	Infrared and Raman	5	1	1	2	1
$E''$	Raman	6	1	2	1	2

<sup>a</sup> The E frequencies are doubly degenerate and each E frequency corresponds to two modes of vibration.

This classification of frequencies based on selection rules for the  $D_{3h}^4=C\bar{6}2c$  space group enables one to obtain a tentative assignment of all observed frequencies (table 7) and to understand why the observed spectrum for tridymite is simpler than that found for both quartz and cristobalite. In particular it explains the observation that only one frequency is observed in the  $850$  to  $625\text{ cm}^{-1}$  region of the spectrum corresponding to a stretching mode associated with motion of the Si atoms.

Although the actual symmetry is lower this indicates that the deviation from  $D_{3h}$  selection rules is apparently not enough to cause a significant change

in the appearance of the infrared spectrum. A more detailed analysis of the spectrum could be made if a Raman spectrum were available. It is interesting that the three observed frequencies in tridymite corresponding to an antisymmetric Si-O stretching, a Si stretching, and to a characteristic mixed O-Si-O and Si-O-Si bending, respectively, appear near the same  $\text{cm}^{-1}$  values in quartz, cristobalite, and coesite indicating that they may be classified as characteristic group frequencies. The mixed-bending frequency observed at  $478 \text{ cm}^{-1}$  corresponds to a frequency close to that observed for cristobalite. The slightly lower values observed in quartz and coesite are interpreted as being due to the change of angle of the tetrahedral units from  $180^\circ$ .

TABLE 7. Classification of observed infrared frequencies of tridymite on the basis of  $D_{3h}$  selection rules

Species <sup>a</sup>	$\text{cm}^{-1}$	Type
$A_2''$ -----	478	Si-O bending.
$E''$ -----	508	Si-O bending.
$E''$ -----	792	Si stretching.
$A_2'$ -----	1,109	Si-O stretching.
$E'$ -----	1,175	Si-O stretching.
$A_2'$ -----	1,175	

<sup>a</sup> The E frequencies are doubly degenerate and each E frequency corresponds to two modes of vibration.

### 3.4. Vitreous Silica

The infrared spectrum of vitreous silica is given in figure 5. The spectrum is characterized by the presence of strong bands at  $1,108 \text{ cm}^{-1}$ ,  $805 \text{ cm}^{-1}$ , and  $468 \text{ cm}^{-1}$  and may be assigned as the Si-O stretching, Si stretching, and Si-O-Si bending characteristic group frequencies, respectively. These frequencies are at essentially the same positions as in the other  $\text{SiO}_2$  modifications, but they are somewhat broader. The broad peak near  $805 \text{ cm}^{-1}$  has its peak absorption at slightly higher  $\text{cm}^{-1}$  values than the other polymorphs of  $\text{SiO}_2$ . This would indicate that there again is no change in the coordination of the tetrahedral units. The broadening of the bands may be due to the random packing of the tetrahedral units. The infrared spectrum of vitreous silica resembles tridymite in appearance with the same number of observed frequencies.

### 3.5. $\text{GeO}_2$

The infrared spectra of three different modifications of  $\text{GeO}_2$  are given in figures 6, 7, 8, 14, and 15, corresponding to the tetragonal, hexagonal, and vitreous forms. The tetragonal form has a rutile structure with two  $\text{GeO}_2$  groups per unit cell, corresponding to sixfold octahedral coordination. The hexagonal form has a quartz-type structure with three  $\text{GeO}_2$  groups per unit cell, corresponding to a tetrahedral coordination. This difference in coordination results in a large difference in frequency of the Ge-O-Ge antisymmetric stretching mode of vibration observed in both spectra. In tetragonal  $\text{GeO}_2$  this frequency is at  $720 \text{ cm}^{-1}$ , whereas in hexagonal quartz-like  $\text{GeO}_2$  it is found at  $885 \text{ cm}^{-1}$ ,

a difference of  $165 \text{ cm}^{-1}$ . This difference is due to the markedly different Ge-O bond length and bond energy for the two forms. For tetragonal  $\text{GeO}_2$ , the Ge-O bond length [3] is  $1.86 \text{ \AA}$ . The bond length for the hexagonal  $\text{GeO}_2$  has not been given, but it is likely that it is shorter than  $1.86 \text{ \AA}$ , corresponding to a stronger bond and larger bond-stretching force constant and vibrational frequency. The large difference in the Ge-O-Ge antisymmetric stretching frequency for those two forms of  $\text{GeO}_2$  is in marked contrast to the positions of the Si-O-Si antisymmetric stretching frequency for the various forms of silica. There is only a small shift in the position of this frequency for the various forms of  $\text{SiO}_2$  indicating that there is no change of coordination and no, or only minor, changes in Si-O bond lengths, bond energies, and bond stretching force constants. The difference in structure of the various forms of silica must be associated with the packing of the tetrahedral units.

The selection rules [8] for a tetragonal  $\text{GeO}_2$  structure with  $D_{4h}^{14} = P4/mnm$  space-group symmetry and two  $\text{GeO}_2$  groups per unit cell predict the presence of six infrared active fundamental frequencies ( $3 A_{2u}$  and  $3 E_u$ ). The observed frequencies and assignment are given in table 8. The three frequencies of species  $A_{2u}$  have been classified as antisymmetric Ge-O stretching, a Ge-O bending, and a low-frequency distortion mode. The first two modes have been assigned to the peaks observed at  $720$  and  $513 \text{ cm}^{-1}$ . The third mode of species  $A_{2u}$  is expected in the regions  $125$  to  $200 \text{ cm}^{-1}$  and would not be observed with the instruments used in this research. The three frequencies of species  $E_u$  have been classified as a Ge-O stretching, a Ge stretching, and a Ge-O bending, and are assigned at  $720$ ,  $525$ , and  $425 \text{ cm}^{-1}$ , respectively. No attempt will be made to explain the shoulders appearing on the  $425 \text{ cm}^{-1}$  band.

TABLE 8. Classification of the observed infrared frequencies of tetragonal  $\text{GeO}_2$

Species <sup>a</sup>	$\text{cm}^{-1}$	Type
$A_{2u}$ -----	-----	Distortion.
$E_u$ -----	425	Ge-O bending.
$A_{2u}$ -----	513	Ge-O bending.
$E_u$ -----	515	Ge stretching.
$A_{2u}, E_u$ -----	720	Ge-O stretching.

<sup>a</sup> Each E frequency is doubly degenerate and corresponds to two modes of vibration.

A detailed interpretation of hexagonal  $\text{GeO}_2$  would require the obtaining of an infrared spectrum run at lower frequencies as well as a Raman spectrum. However, the observed spectrum is consistent with that found for low-temperature quartz. The strong peak at  $885 \text{ cm}^{-1}$  is clearly the analogue of the  $1,100 \text{ cm}^{-1}$  Si-O-Si antisymmetric stretching frequencies of quartz in species B and E and must consist of two fundamental frequencies. The  $801 \text{ cm}^{-1}$  and  $782 \text{ cm}^{-1}$  peaks of quartz correspond to the Si stretching modes and would be expected to shift markedly in hexagonal  $\text{GeO}_2$  because of the heavier mass of the Ge atom. Tentatively these two peaks

TABLE 9. Classification of the observed infrared frequencies for hexagonal GeO<sub>2</sub> (cm<sup>-1</sup>)

Species	GeO <sub>2</sub>	Type	Quartz assignment
A (Raman active)	-----	-----	-----
B (Infrared active)	345	Distortion -----	374
	515	Ge-O bending -----	513
	885	Ge stretching -----	780
		Ge-O stretching -----	1, 150
	-----	-----	128
	585	Ge stretching -----	397
			696
E (Infrared active)	963	Ge-O stretching -----	1, 176
	332	-----	265
	540	Ge-O bending -----	462 to 475
	885	Ge-stretching -----	801
		Ge-O stretching -----	1, 097

of quartz will be respectively associated with the peaks of hexagonal GeO<sub>2</sub> at 540 cm<sup>-1</sup> and 515 cm<sup>-1</sup>. The first of these has been assigned to species E and the latter to species B of the quartz structure. The 696 cm<sup>-1</sup> band of quartz must then be shifted to 585 cm<sup>-1</sup> in GeO<sub>2</sub> and assigned to species E. The two remaining frequencies observed in hexagonal GeO<sub>2</sub> at 345 cm<sup>-1</sup> and 332 cm<sup>-1</sup> must be considered as the analogs of the mixed Si-O-Si, O-Si-O bending frequencies observed in quartz at 513 cm<sup>-1</sup> and 462 cm<sup>-1</sup>, respectively. The first (345 cm<sup>-1</sup>) must be assigned to species B, and the second (332 cm<sup>-1</sup>) to species E of

the quartz structure. This assignment is given in table 9.

The Ge-O-Ge antisymmetric stretching of vitreous GeO<sub>2</sub> is found at 895 cm<sup>-1</sup> as a broad band and indicates its similarity with hexagonal GeO<sub>2</sub> in that both consist of tetrahedrally coordinated GeO<sub>2</sub> units. No additional low-frequency bands were observed in fused GeO<sub>2</sub>.

#### 4. References and Notes

- [1] B. D. Saksena, Proc. Indian Acad. Sci., [A] **12**, 93 (1940); R. S. Krishnan, Nature **155**, 452 (1945); J. Barriol, J. Phys. Radium **7** [8], 209 (1946); F. Matossi, J. Chem. Phys. **17**, 679 (1949); R. C. Lord and J. C. Morrow, J. Chem. Phys. **26**, 230 (1957); I. Simon and H. O. McMahon, J. Chem. Phys. **21**, 23 (1953). These references contain references to earlier work on the Polymorphs of SiO<sub>2</sub>.
- [2] L. Coes, Jr., Science **118**, 131 (1953); R. B. Sosman, Science **119**, 738 (1954).
- [3] A. W. Laubengayer and G. S. Morton, J. Am. Chem. Soc. **54**, 2303 (1932).
- [4] W. Zachariasen, Z. Krist. **67**, 226 (1928).
- [5] J. J. Kirkland, Anal. Chem. **27**, 1537 (1955).
- [6] R. W. G. Wyckoff, Z. Krist. **62**, 189 (1925).
- [7] T. F. W. Barth, Am. J. Sci. **23**, 350 (1932); **24**, 102 (1932).
- [8] For a discussion of vibrational selection rules and vibrational species see G. Herzberg, Infrared and Raman Spectra, D. Van Nostrand Co. (1945).
- [9] R. E. Gibbs, Proc. Roy. Soc. [A] **113**, 351 (1927).

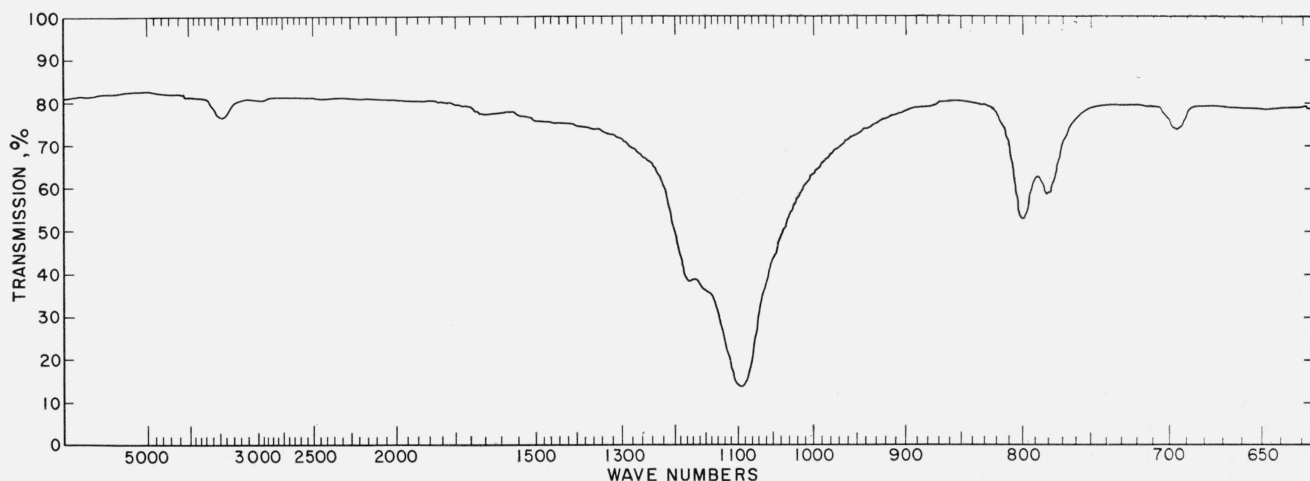


FIGURE 1. Infrared transmission spectrogram of quartz from Lisbon, Md.

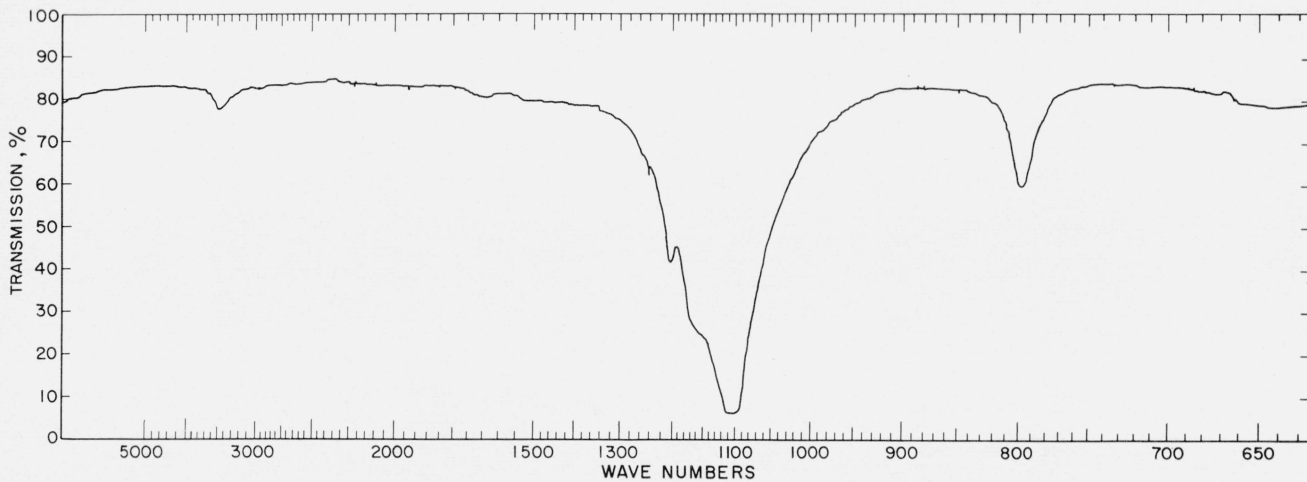


FIGURE 2. *Infrared transmission spectrogram of cristobalite.*

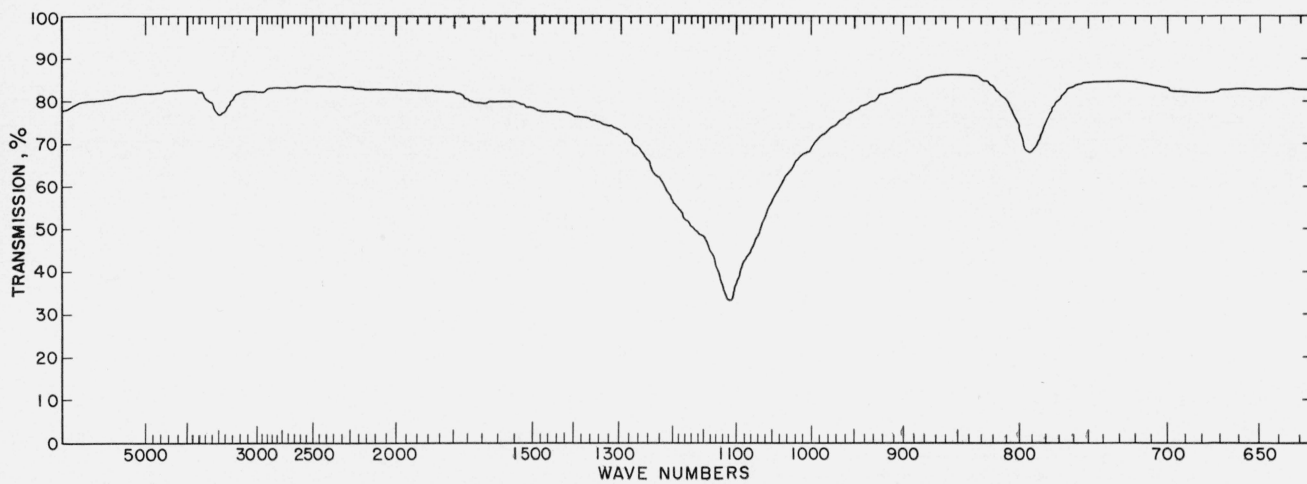


FIGURE 3. *Infrared transmission spectrogram of tridymite.*

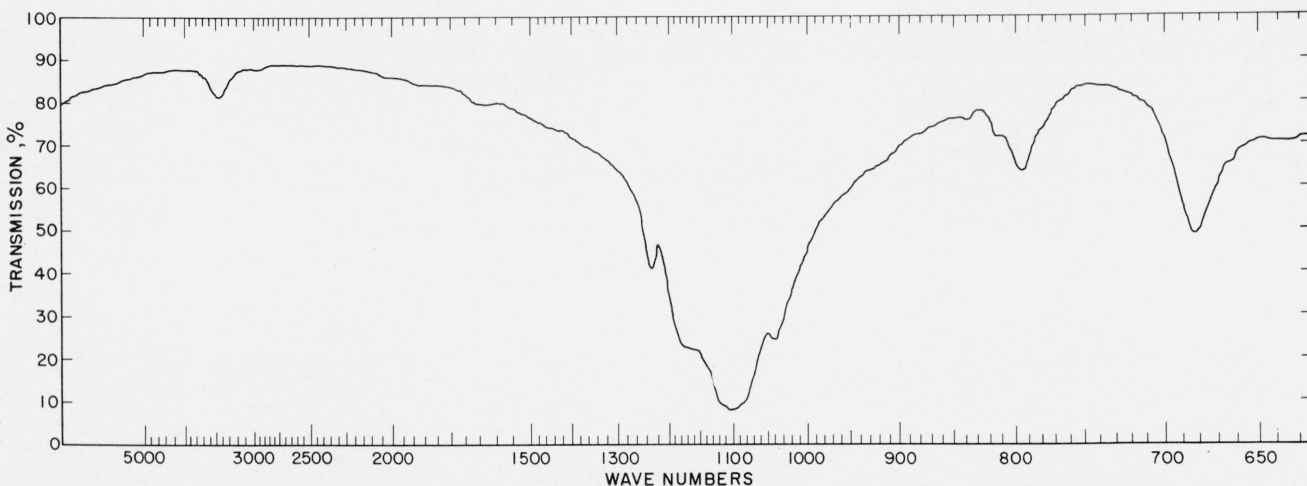


FIGURE 4. *Infrared transmission spectrogram of coesite.*

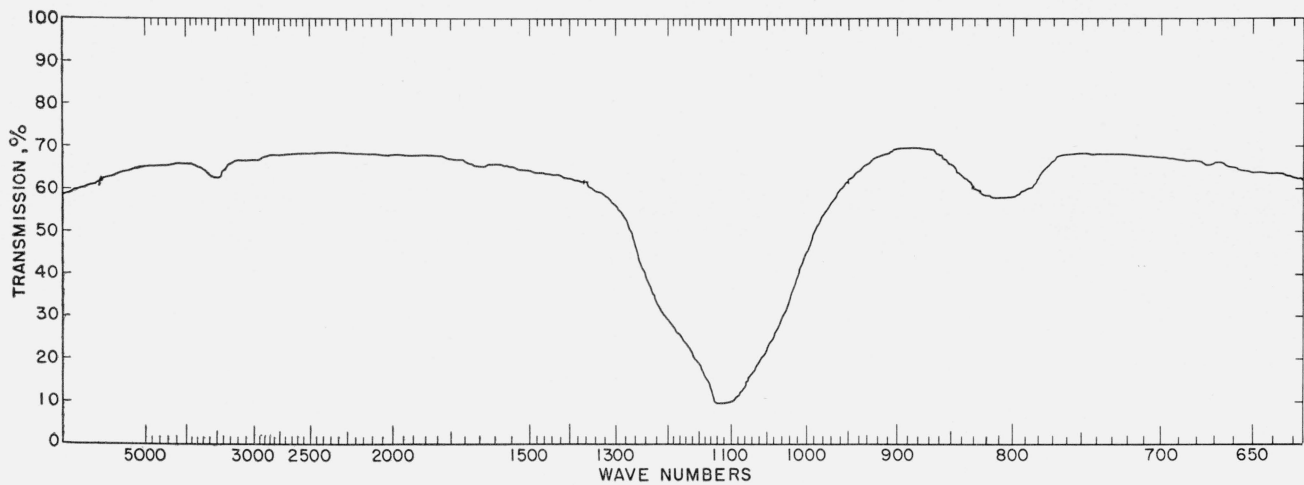


FIGURE 5. *Infrared transmission spectrogram of vitreous SiO<sub>2</sub>.*

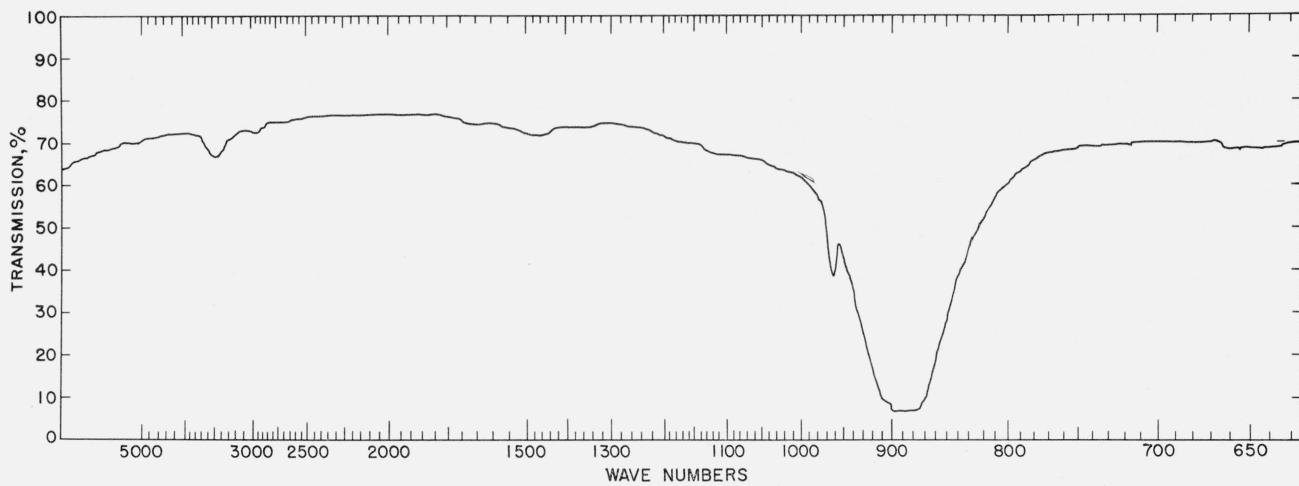


FIGURE 6. *Infrared transmission spectrogram of hexagonal GeO<sub>2</sub>.*

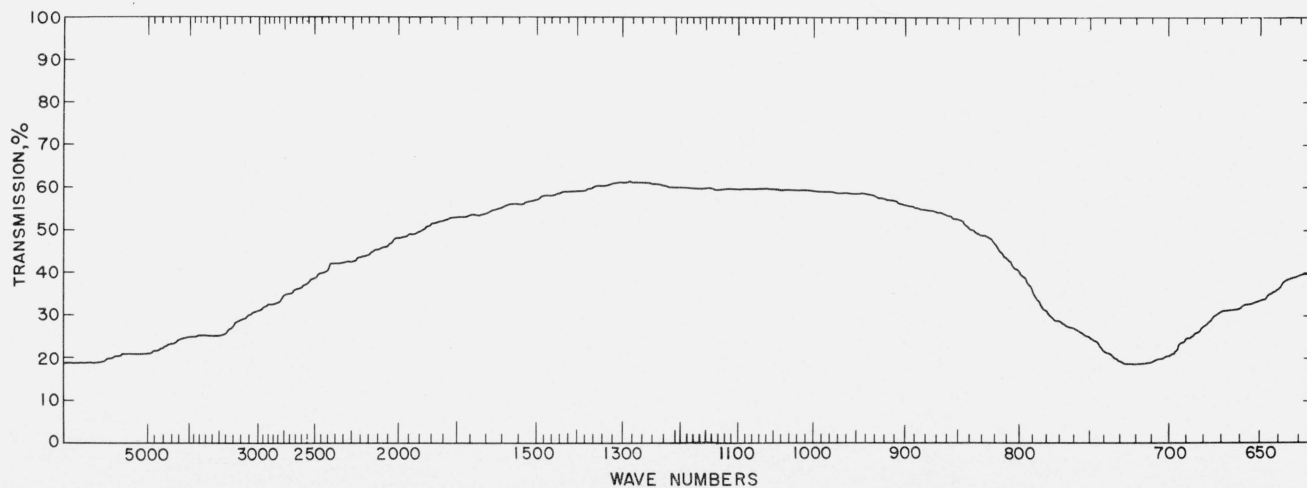


FIGURE 7. *Infrared transmission spectrogram of tetragonal GeO<sub>2</sub>.*



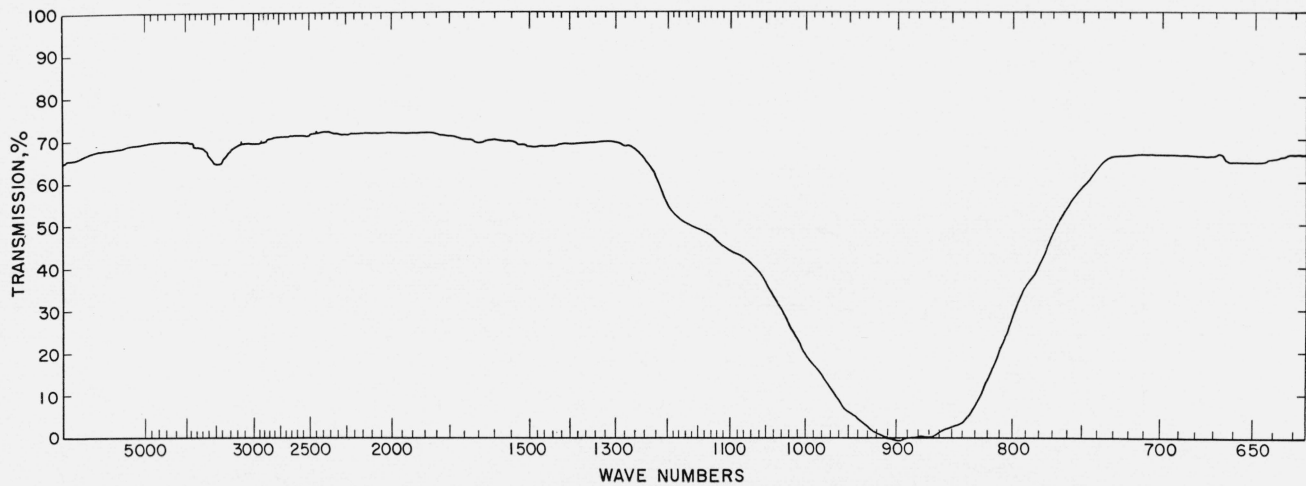


FIGURE 8. *Infrared transmission spectrogram of vitreous GeO<sub>2</sub>.*

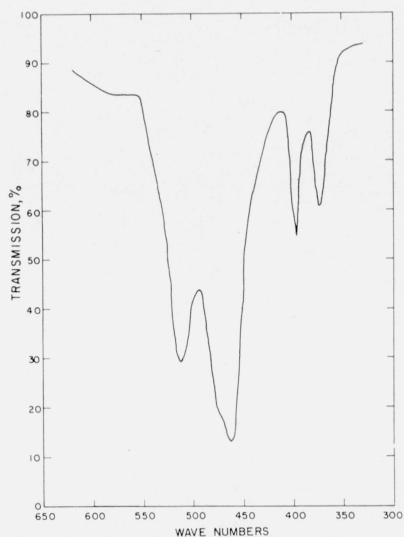


FIGURE 9. *Infrared transmission spectrogram of quartz.*

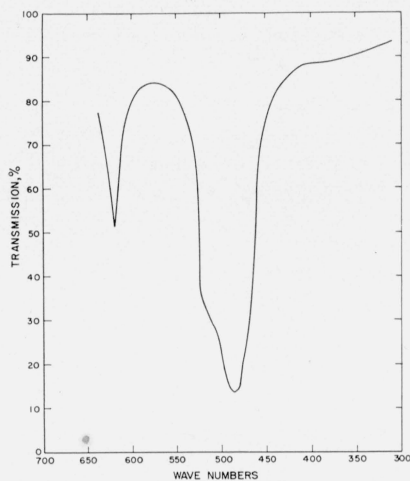


FIGURE 10. *Infrared transmission spectrogram of cristobalite.*

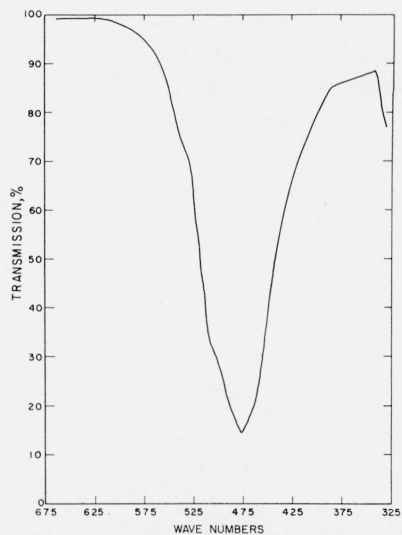


FIGURE 11. *Infrared transmission spectrogram of tridymite.*

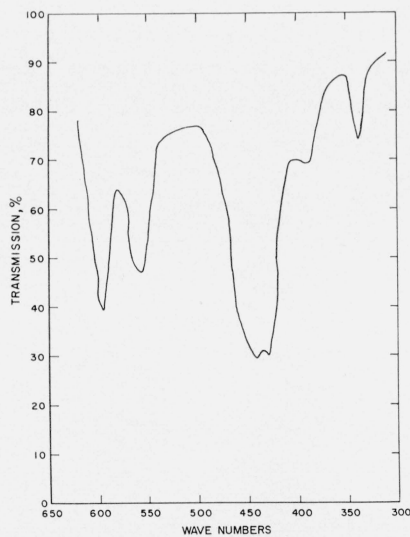


FIGURE 12. *Infrared transmission spectrogram of coesite.*

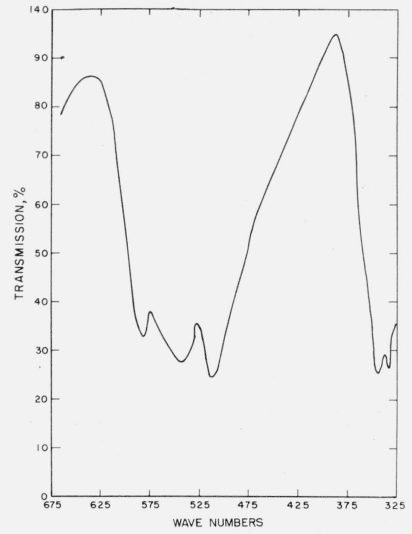
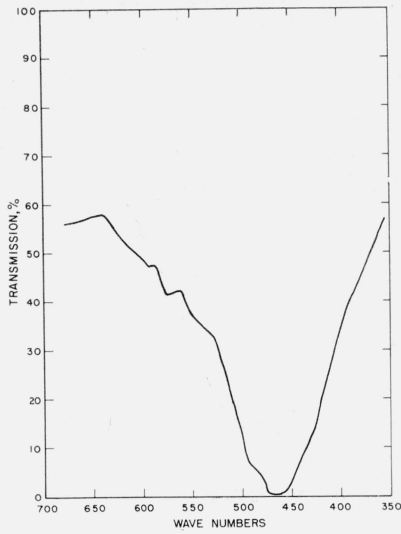


FIGURE 13. *Infrared transmission spectrogram of vitreous SiO<sub>2</sub>.*

FIGURE 14. *Infrared transmission spectrogram of hexagonal GeO<sub>2</sub>.*

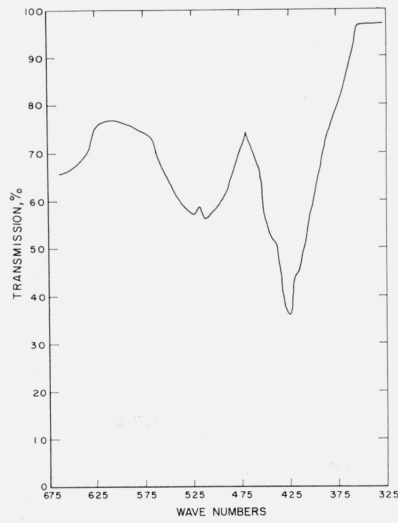


FIGURE 15. *Infrared transmission spectrogram of tetragonal GeO<sub>2</sub>.*

WASHINGTON, March 28, 1958.

○